



---

Yan, B, Bai, W, Qian, L and Ma, Z (2018) Study on hydro-kinematic characteristics of green water over different fixed decks using immersed boundary method. Ocean Engineering, 164. pp. 74-86. ISSN 0029-8018

---

**Downloaded from:** <https://e-space.mmu.ac.uk/620824/>

**Publisher:** Elsevier

**DOI:** <https://doi.org/10.1016/j.oceaneng.2018.06.037>

**Usage rights:** Creative Commons: Attribution-Noncommercial-No Derivative Works 4.0

Please cite the published version

<https://e-space.mmu.ac.uk>

# Study on hydro-kinematic characteristics of green water over different fixed decks using immersed boundary method

Bin Yan<sup>a</sup>, Wei Bai<sup>b,\*</sup>, Ling Qian<sup>b</sup>, Zhihua Ma<sup>b</sup>

<sup>a</sup>*Department of Civil and Environmental Engineering, National University of Singapore, Kent Ridge, Singapore 117576, Singapore*

<sup>b</sup>*School of Computing, Mathematics and Digital Technology, Manchester Metropolitan University, Chester Street, Manchester M1 5GD, UK*

---

## Abstract

An immersed boundary method is applied to simulate the green water over a fixed deck by combining a level set method for the free water surface capturing. An efficient Navier-Stokes equation solver of second-order accuracy adopting the fractional step method at a staggered Cartesian grid system is used to solve the incompressible fluid motion. The numerical model is validated by comparing extensively the wave elevation and pressure with the experimental data for two types of fixed decks, which suggests that the developed immersed boundary method coupled with the level set method is very promising to predict green water problems due to its accuracy and efficiency. Furthermore, the cross-sectional velocity distribution over the deck, which is an important parameter in the industrial application, is computed and compared to the analytical Ritter's solution. It is found that Ritter's solution is much more conservative than the numerical simulations, which confirms the safe application of the simplified analytical solution in the current design practise. Volume of green water over the deck that affects the stability of deck is also tracked. The numerical results reveal that the amount of green water over both the two types of fixed decks shows a linear relationship with the relative wave height. This important finding may be very helpful for the prediction of deck elevation under a certain wave condition to reduce the occurrence of green water event.

*Keywords:* Green water, Immersed boundary method, Level set method, FPSO and platform decks, Cross-sectional velocity, Water volume

---

## 1. Introduction

Green water impact is a hazardous event in ocean and coastal engineering that could cause local damage and global failure of marine vessels and offshore platforms. In high sea states, when big waves impact at ships and platforms, a part of the water runs up along the vertical surface of the structure, collapses onto the frontal deck violently and quickly washes over the whole deck. As the wave breaks and overtops on a marine

---

\*Corresponding author  
Email address: w.bai@mmu.ac.uk (Wei Bai)

structure, the flow becomes multi-phased and sometimes chaotic in the fluid area close to the structure, which makes the green water problem more complicated and challenging.

For simple cases, some analytical solutions have been derived for the green water problem in the past. For instance, a simplest solution to green water with the assumption of a frictionless dry flat bed was proposed in Ritter (1892), in which the free surface profile for a collapsing rectangular column of fluid over a horizontal bed was described. This analytical solution has been widely used in the industry for green water predictions. However, experimental and analytical study in Lauber and Hager (1998) on the dam break indicated that the front velocity of a dam break flow reduces as time increases, which disagrees with the constant front velocity shown in the analytical solution of Ritter (1892). In recent years, a semi-analytical solution was developed in Yilmaz et al. (2003) for a dam break flow to simulate the green water problem. The result indicated that a jet-like water profile can be formulated at the forefront of the flow. However, the analytical solution is still too simple to fully elucidate the physics of green water over a deck.

French (1969) carried out the early experiments to investigate the vertical force due to the regular wave slamming on a horizontal plate. An impulsive force was captured in the experiments. Another experiment was conducted in Denson and Priest (1971) to identify the influence of relative wave height, relative plate clearance, relative plate width and relative plate length on the pressure distribution under a thick horizontal plate. A potential flow model was also developed in Lai and Lee (1989) to predict the vertical forces caused by large amplitude waves on decks. Their numerical results were consistent with the experimental results in French (1969). In addition, Kaplan (1992) extended the hydrodynamics theory for ship slamming to study the wave action on a deck slab by representing the time varying vertical forces as the combination of a hydrodynamic impact force and a drag force. The time history of vertical forces indicated that the force magnitudes are considerably large, but a discontinuity appears at the instant of complete submergence of the structure. Cox and Scott (2001) and Cox and Ortega (2002) conducted the experimental study on the green water over a fixed deck in a narrow wave flume. In Cox and Scott (2001) it was found that free surface and volumetric overtopping exceedance probability follow the exponential distributions. Cox and Ortega (2002) experimentally revealed that the wave collapsing into a thin deck exhibits the velocities that exceed 2.4 times the maximum crest velocity in the case without the deck.

Based on the experiment in Cox and Ortega (2002), green water over a fixed deck was analyzed using the Smoothed Particle Hydrodynamics (SPH) method in Gómez-Gesteira et al. (2005). The numerical results of wave profile agreed well with the experimental data, in both phase and amplitude. In addition, with the incompressible SPH model Shao et al. (2006) investigated the overtopping phenomenon on a fixed deck caused by a transient wave. The results were in good agreement with the experimental and other numerical data. As the CFL condition was completely related to the fluid particle velocity, a much larger time step could be adopted in Shao et al. (2006) than that used in Gómez-Gesteira et al. (2005). Still based on the experiment in Cox and Ortega (2002), a finite element Navier-Stokes solver combining with a single-phase Volume of Fluid (VOF) technique was developed in Lu et al. (2010) to investigate the green water phenomena

on a fixed deck, and a deck-house on a floating structure. In the recent work of Qin et al. (2017), green water on rigid deck, elastic bare deck and elastic deck with intermediate elastic supports caused by freak waves and the deck response were studied.

Besides the studies on green water over a thin deck, Greco (2001) conducted an important experimental investigation of two-dimensional green water on the deck of a fixed Floating, Production, Storage and Offloading (FPSO) vessel model without and with a solid wall. Two green water events as well as two peaks in the green water height and pressure on the solid wall were observed. An air cavity was also captured when the green water travelled along the deck. In the numerical simulation based on the potential flow model presented in Greco (2001), the free surface evolution was in reasonable agreement with the physical observation just for the lower wave steepness. Barcello et al. (2003) carried out the experiments for stationary vessel models in head waves to study the characteristics of green water loads and water-front velocity on the deck. Both the pressure on the deck and the horizontal force on the wall show a double-peaked evolution, which is similar to those in Greco (2001). Based on the experimental work in Greco (2001), Nielsen and Mayer (2004) simulated green water on a vessel with and without motions by the use of a Navier-Stokes flow solver with the VOF scheme. The water elevation on the two-dimensional deck agreed well with the data in Greco (2001), but the extension to the three-dimensional situations indicated that the three-dimensional effect is insignificant.

More recently, Ryu et al. (2007a,b) compared the green water with the dam break flow to examine the applicability of dam break flow models to describe green water flows. The comparisons indicated that the solution of Ritter (1892) for dam break flows works well in the prediction of green water velocity despite the significant difference between these two flows. In addition, the green water over three different structures in regular head waves were presented experimentally in Lee et al. (2012), based on which a database for the validation of numerical simulations was developed. Ariyaratne et al. (2012) found the relationship among impact pressure, wave celerity, and air void in the experiment of green water over a three-dimensional deck. Furthermore, Xiao et al. (2014, 2015) conducted an experimental study on the green water along the broadside of a single-point moored FPSO vessel in oblique waves. The comparison among three types of deck revealed that the elasticity of the deck affects the local fluid pressures significantly. Silva et al. (2017) also simulated the beam and quartering wave on the deck by customizing the commercial CFD code ANSYS FLUENT®.

From the above discussion, it is observed that all the previous work mainly focused on the investigation of water surface elevation, green water loads and pressure distribution over the deck. The lack of understanding of other hydrodynamic characteristics during the green water event demands more research on the problem. As the wave impact on the deck could threaten the safety of topside structures as well as human life on the deck, during engineering designs the velocity of wave on the deck is required when a Morison-type of equation is adopted to calculate the impact force caused by wave on deck (Bea et al., 1999 and Kaplan, 1992). On the other hand, the volume of green water on deck is of significant engineering interest, which leads to much

additional load on the deck when worst case scenario happens in the extreme situation. Therefore, the present study aims at obtaining the deep insight into some important hydrodynamic features, such as the velocity distribution over the deck and volume of green water, when the green water impacts on different decks. To achieve this, a developed immersed boundary method in conjunction with a level set method is extended to study the green water over both the FPSO deck and platform deck, after the extensive validation through the comparison of water surface elevation and pressure with the physical experiments. This numerical model is based on an improved immersed boundary method developed in Yan et al. (2018), where a new and simpler forcing point searching scheme was proposed. The obtained cross-sectional velocity distribution over the deck is compared with the analytical solution that is being widely used in the industry for the green water problem, and the applicability of this simplified solution is evaluated. More importantly, the amount of green water on different decks is also examined, which may be difficult to estimate experimentally. A relationship between the green water volume and the relative incident wave height is identified.

## 2. Mathematical formulation

### 2.1. Governing equations

For two-dimensional incompressible viscous flows, the fluid motion can be described by the Navier-Stokes equations,

$$\frac{\partial u_i}{\partial t} + u_j \frac{\partial u_i}{\partial x_j} = \frac{1}{\rho} \left( -\frac{\partial p}{\partial x_i} + \frac{\partial \tau_{ij}}{\partial x_j} \right) + g_i + f_i, \quad (1)$$

and the continuity equation,

$$\frac{\partial u_i}{\partial x_i} = 0, \quad (2)$$

where  $u_i$  is the fluid velocity,  $p$  is the pressure,  $x_i$  is the spatial coordinate,  $t$  is the time,  $g_i$  is the gravitational acceleration,  $\rho$  is the fluid density and  $\tau_{ij}$  are the viscous stress components. Here the Cartesian tensor notation is used, and  $f_i$  is the momentum forcing component to enforce the desired boundary condition on an immersed boundary interface.

The flow governed by the Navier-Stokes equations is solved by a finite difference method on a staggered grid system. With a second-order Runge-Kutta Total Variation Diminishing (RK-TVD) scheme for the discretization of the temporal gradient, the Navier-Stokes equations can be decoupled and solved by a fractional step method (see Archer and Bai, 2015 for more details).

### 2.2. Free surface simulation

To simulate flows with the free surface undergoing topological changes, splitting and merging, the air-water interface is captured by the level set method. In the level set method, we define a scalar distance

function  $\phi$  in the whole domain to measure the shortest distance between the grid cell and the interface, and the function  $\phi$  follows a convective equation,

$$\frac{\partial \phi}{\partial t} + u_i \frac{\partial \phi}{\partial x_i} = 0. \quad (3)$$

With the spatial gradient of  $\phi$  in Eq. 3 discretized by a fifth-order HJ-WENO scheme (Jiang and Peng, 2000), the values of  $\phi$  can be updated by a third-order RK-TVD scheme. The detailed numerical implementation can be found in Archer and Bai (2015).

### 2.3. Immersed boundary method

In the immersed boundary method, the body boundary condition is represented by the momentum forcing component in Eq. 1. Since the solid body surface may not be coincident with computational nodes in the staggered grid system, the imposed forcing component has to be calculated at the corresponding node (termed as the forcing point) nearest to the immersed solid boundary. Therefore, the forcing points should be found first. To demonstrate the searching of forcing point, the line segment  $x_1$ - $x_2$  shown in Fig. 1 represents a boundary, and the shadowed area in the figure indicates the solid phase. In the searching process, an imaginary Lagrangian point travels from Point  $x_1$  along the line segment towards Point  $x_2$ . When the Lagrangian point meets the first vertical grid line, the intersection between the line segment and vertical grid line is recorded. The  $u$  velocity position nearest to the intersection in the fluid phase is then identified and defined as a  $u$  forcing point. The Lagrangian point continues to travel by a half grid in the  $x$  direction, such that it locates on the same vertical line with the  $v$  velocity position. Along this vertical line, the nearest  $v$  velocity position in the fluid phase is recorded as a  $v$  forcing point. When the Lagrangian point eventually reaches Point  $x_2$ , all required forcing point information can be gathered (see Yan et al., 2018 for more details).

After the location of forcing point is determined, the forcing component at the forcing point is predicted based on the method described in Mohd-Yusof (1997). When the forcing point happens to locate on the solid boundary, such as Point A in Fig. 1, the forcing term can be simply predicted by

$$f_i = \frac{v_A - v_i^n}{\Delta t} - RHS_i^n, \quad (4)$$

where  $RHS$  includes all the convective, viscous, pressure gradient and body force terms in the governing equations, the superscript  $n$  denotes the value at the previous time step, and  $v_A$  is the velocity on the body surface. This forcing term is directly calculated since the desired boundary condition can be satisfied exactly but only hold for this special situation. In the more general situations, the forcing point is not located on the boundary surface, such as Point C in Fig. 1. The velocity at the forcing point,  $u_f$ , has to be constructed using the information from the boundary condition and surrounding flow field. For instance,  $u_f$  at Point C can be determined by the linear interpolation from the velocities at Points B and D, where the velocity

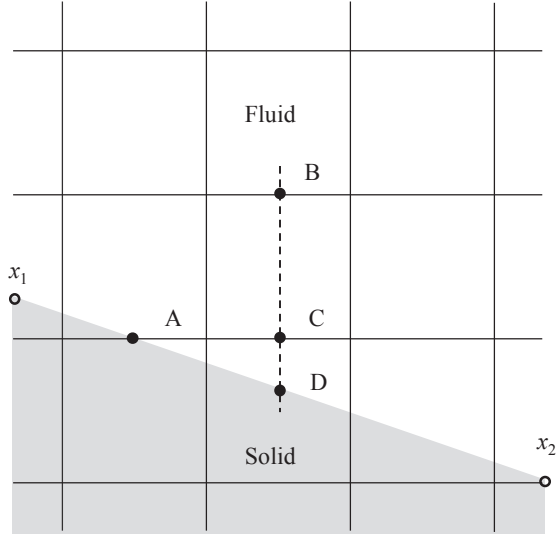


Figure 1: Illustration of the location and determination of imposed forcing component

at Point D comes from the body boundary condition. With the predicted velocity at the forcing point, the forcing term at the forcing point can be expressed as

$$f_i = \frac{v_f - v_i^n}{\Delta t} - RHS_i^n. \quad (5)$$

### 3. Green water on a fixed FPSO deck

The problem of green water can be classified into two categories according to the body geometry: green water on ships or vessels; and green water on platforms. In order to make the numerical simulation feasible, appropriate simplifications are always adopted, while retaining most of the physics of the problem. The problem of green water on vessels (such as the FPSO structure) can be simplified by wave interaction with a rectangular box, as adopted in Greco (2001), which is studied in this section. On the other hand, the problem of green water on offshore platforms (such as the jack-up or tension leg platform) can be simplified as wave action on a horizontal plate, where all supporting structures are ignored (Cox and Ortega, 2002); this problem will be investigated in the next section.

#### 3.1. Comparisons with experiment

Based on the experiment in Greco (2001), numerical simulations are conducted for the green water on a fixed FPSO deck to determine the accuracy of the present model. A sketch of the setup in numerical simulations is shown in Fig. 2, which is the same to the experiment in Greco (2001). In the numerical simulations, the wave elevations in the tank are recorded by two wave probes, *WP1* and *WP2*, which locate

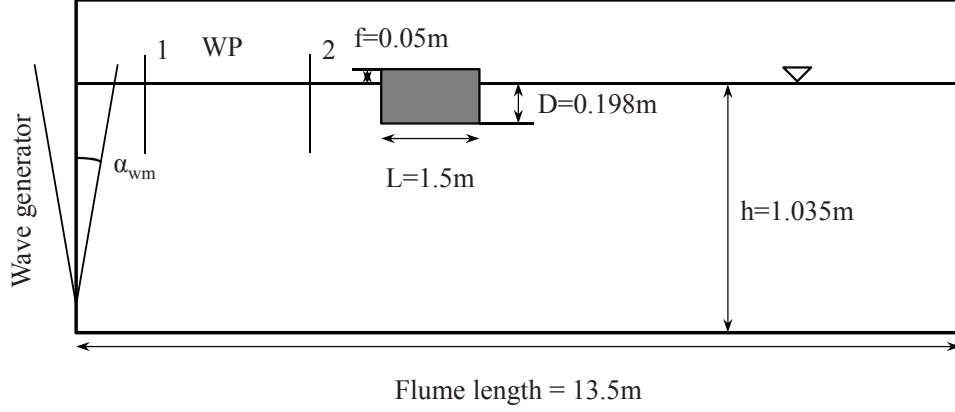


Figure 2: Sketch of the problem of wave on a rectangular deck

152 0.79m and 5.436m away from the neutral position of the flap wave maker, respectively. The leading edge  
 153 of the deck is 5.54m from the wave maker (also see other geometric information in Fig. 2). In addition,  
 154 both the experiment and numerical simulation also consider the situation that a vertical wall is introduced  
 155 at 0.2275m from the bow, as shown in Fig. 3. In this case, three wave probes spaced 0.075m between each  
 156 other are placed on the top of the deck, namely WL1, WL2 and WL3. Meanwhile, two pressure gauges,  
 157 PR1 and PR2, are mounted on the wall 12mm and 32mm above the deck, respectively.

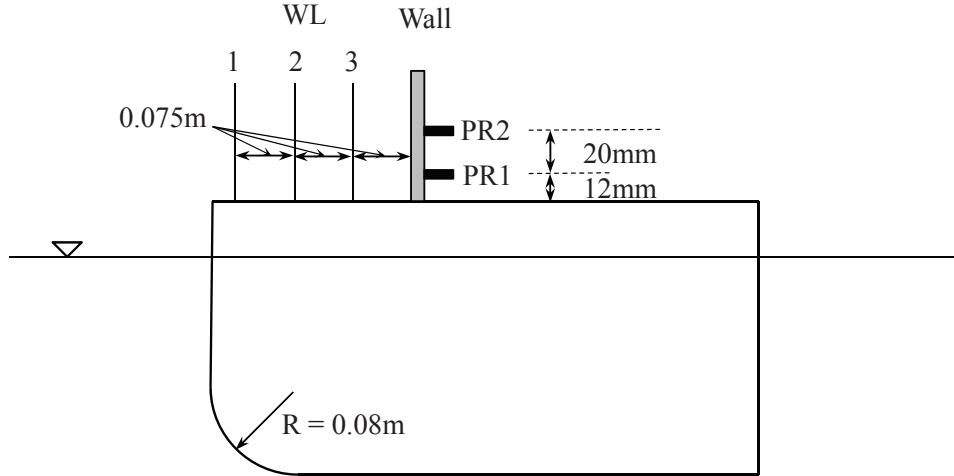


Figure 3: Details around the deck of two-dimensional FPSO

158 The wave parameters are given as follows: wave height  $H = 0.16m$ , wave period  $T = 1.1s$  and wave  
 159 length  $\lambda = 2.0m$ . At the beginning of wave generation, a linear sinusoidal ramp function is introduced  
 160 over the first 2s to give a smooth transition from the calm water, which also avoids the possible unwanted  
 161 resonant waves. In the physical experiment, the angle of the flap was specified as the wave generation signal,  
 162 which is shown in Fig. 4(a). In the present numerical model, the velocity of the flap is required as the input



at the inlet boundary in order to generate waves in the tank. Fig. 4(b) shows the time history of the angular velocity of the flap, which is adopted in the present numerical simulations.

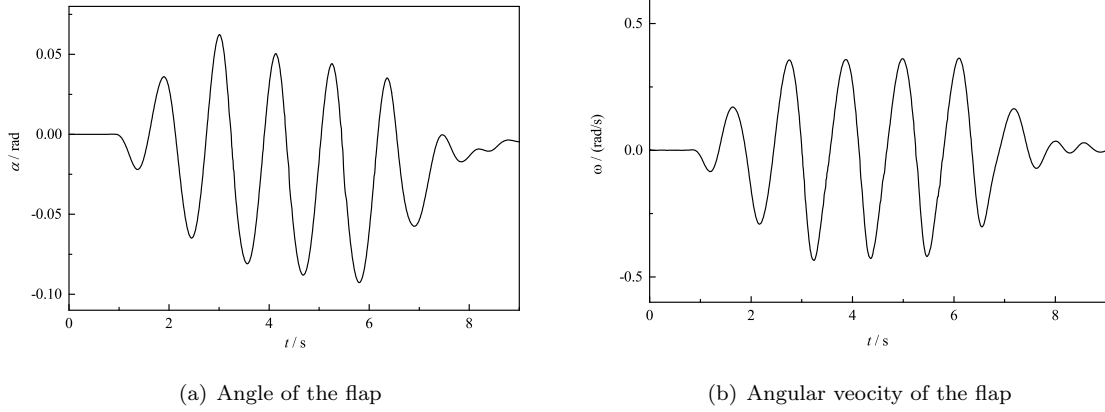


Figure 4: Signal of wave maker motion for generating the incoming wave with  $\lambda = 2m$  and  $H = 0.16m$

To verify the convergence of the simulation of wave on deck, three grids are tested. In the present work, a relatively fine mesh size ( $0.004m$  equivalent to around 50 cells in one wave height) in the vertical direction is imposed around the FPSO deck and wave surface, so that only the mesh size in the horizontal direction needs to be changed to test the convergence. Coarse grid (*Mesh\_1*), medium grid (*Mesh\_2*) and fine mesh (*Mesh\_3*) employ the intervals of  $0.04m$ ,  $0.02m$  and  $0.01m$  respectively in the horizontal direction in the area between the flap and FPSO deck. The time history of wave elevations at the wave probes *WP1* and *WP2* is shown in Fig. 5 for the case without the wall, where the difference between the results at the medium and fine grids is little, while the coarse grid *Mesh\_1* deviates much from the other two. Therefore, the numerical results obtained at *Mesh\_2* are adopted in the following discussion for this problem.

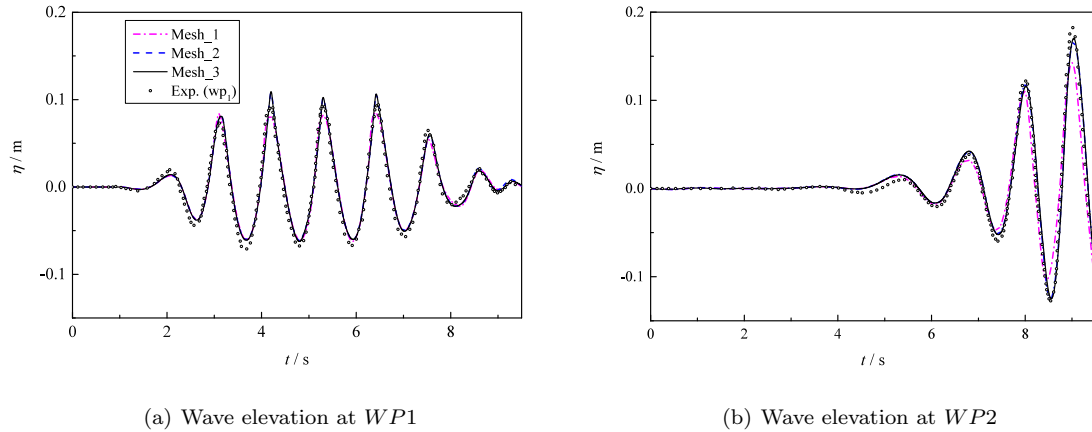


Figure 5: Convergence test of wave elevation with the incident wave height  $H = 0.16m$

At the same time, in Fig. 5 the experimental data of wave elevations at the two wave probes in Greco (2001) is also shown for the purpose of comparison. It can be seen that the agreement is considerably satisfactory, in spite of a little difference observed on the trough and crest. When the wave propagates to the front of the deck, the incoming wave and the reflected wave are superimposed. As a result, the standing wave occurs, so that the wave height shown in Fig. 5(b) is significantly larger than the incident wave height  $H = 0.16m$ .

When the incident wave propagates to the deck, it is reflected from the deck. As a result, standing wave is generated and wave amplitude before the deck is enlarged. It leads to water running up on the deck, known as green water. The green water height over the deck is important, which has a significant influence on the pressure on the deck or vertical wall. Comparison of the resulting water heights on the deck at the three locations  $WL1$ ,  $WL2$  and  $WL3$  is shown in Fig. 6 for the case without the wall. It is noted that there are two wave impact events, of which the second event is significantly higher than the first one, because of the superposition of reflected wave in front of the FPSO deck. It can be seen clearly that the maximum green water heights at the three probes decrease, where the first probe  $WL1$  records the largest values for both the two wave impact events. Furthermore, the wave height at  $WL1$  shows a good consistence to the experimental data, where the first shipping wave occurs at around  $t = 7.0s$ . The second event appears to be almost 2.5 times high as the first one. At the second and third recorders ( $WL2$  and  $WL3$ ), the height of green water also agrees well with the experiment data. However, at the third probe  $WL3$  the second wave front is slightly underestimated compared to the experimental data, which could be due to the numerical dissipation over the larger distance from the bow.

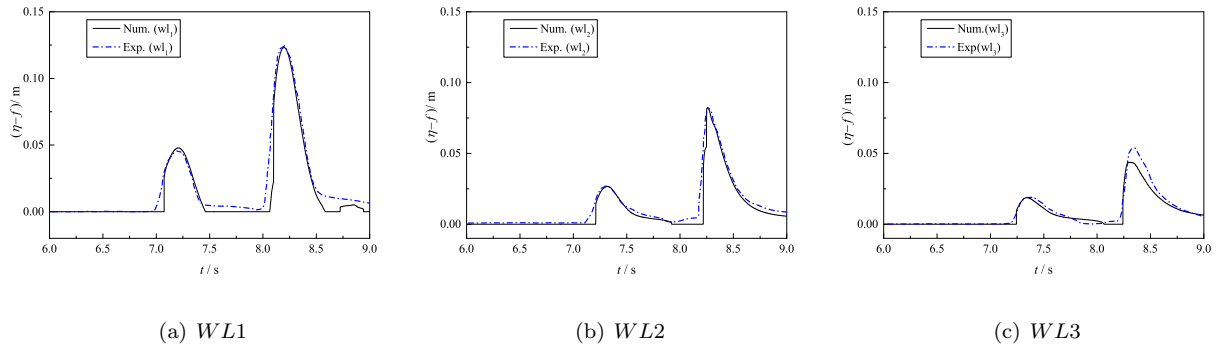


Figure 6: Comparison of water surface measured at three positions with the experimental data, where  $f$  is the elevation of deck above the still water.

When the vertical wall is mounted on the deck, the pressures due to the wave impact at the two locations (see  $PR1$  and  $PR2$  in Fig. 3) are shown in Fig. 7. Generally, the present numerical results agree well with the experimental data in Greco (2001). However, it still can be observed that the numerical results are a little overestimated compared to the experimental data, which might be caused by the fine bubbles in front

of the wall. Those fine bubbles that are capable of dissipating energy, can be captured in the experiment, but demand prohibited computing resources in the numerical simulations with huge amount of finest meshes.

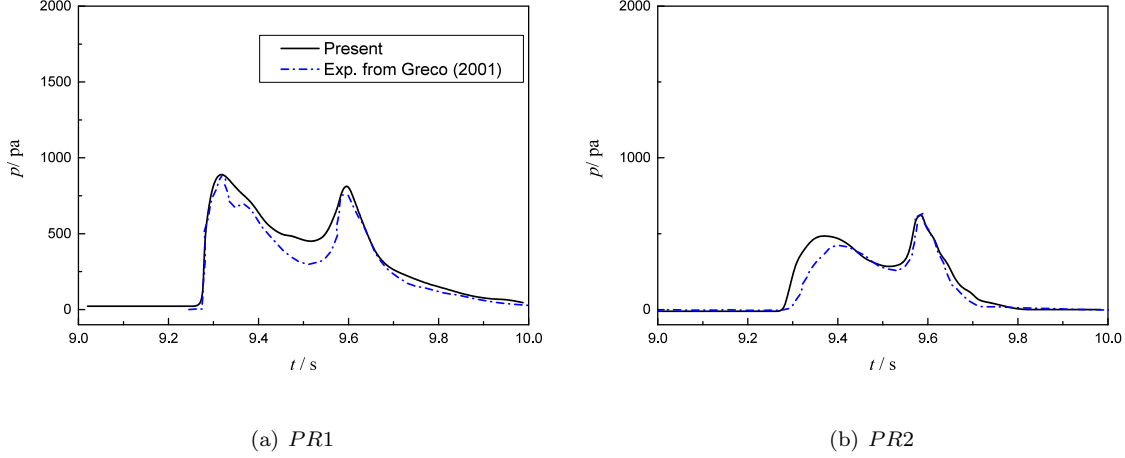


Figure 7: Comparison of pressure recorded at two positions between the present numerical simulation and the physical experiment

### 3.2. Velocity distribution of wave on deck

The horizontal  $u$  velocity distribution in the first impact event for the cases with and without the wall is presented in Fig. 8. From the figure, it is seen that there is little difference between these two cases, and the mounted wall has little influence on the  $u$  velocity distribution, because the green water on the deck has not reached the mounted wall. For the purpose of comparison, the horizontal  $u$  velocity distribution in the second impact event is also presented in Fig. 9. It is obvious that the presence of the mounted wall can change the  $u$  velocity distribution, especially between  $t = 8.96s$  and  $t = 9.20s$ .

It is well known that green water on a marine structure has similarity with a dam break flow; see Buchner (1995) and Ryu et al. (2007b) for more discussion. In fact, a standard design analysis procedure has been developed using the dam break solution to estimate the velocity of a green water event. The analytical solution developed by Ritter (1892) is widely used to predict the cross-sectional velocity  $U_c$  (the average velocity over the whole cross section),

$$U_c(x, t) = \frac{2}{3} \left( \frac{x}{t} + \sqrt{gH_0} \right), \quad (6)$$

where  $x$  is the distance from the deck edge,  $t$  is the time instant measured from when the green water occurs,  $H_0$  is the distance from the maximum wave crest to the deck. In this case, the maximum wave crest of the first event is about 17cm,  $H_0$  is thus 12cm. The numerical results of cross-sectional velocity of green water for the first event along the deck are presented in Fig. 10 for the case without the wall, in which the analytical solution in Ritter (1892) is also included for the comparison. It is noted that the analytical

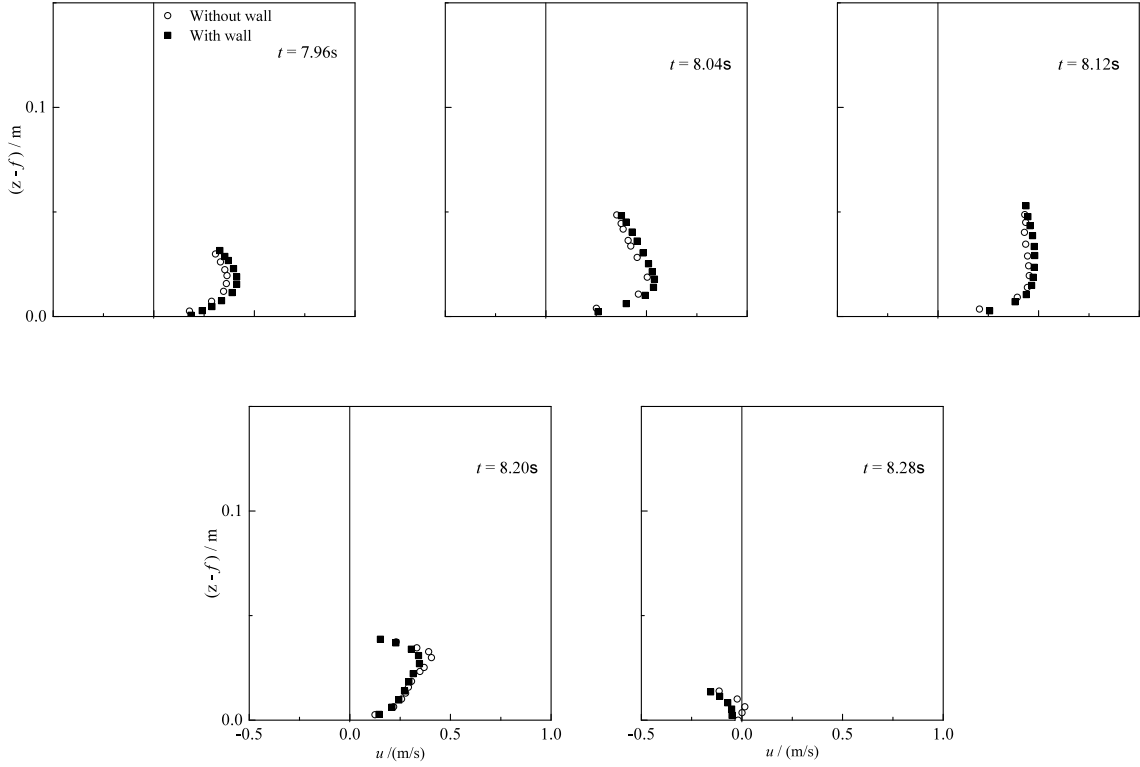


Figure 8: Comparison of  $u$  velocity distribution at the edge of deck for the cases with and without the wall in the first impact event

solution is obviously overestimated at the first four time instants. However, at the last four time instants, the analytical velocity at the water front appears slightly underestimated. Therefore, there is a large discrepancy between the analytical and numerical results, which may be caused by the occurrence of a jet-like formation at the forefront of green water, which appears in the present numerical simulation. This phenomenon has also been observed in Stansby et al. (1998) and Yilmaz et al. (2003). As a result, the analytical solution of Ritter (1892) is too simple to elucidate the physics of green water over a deck clearly. Nevertheless, the analytical solution is more conservative in the most situations and safer to estimate the cross-sectional velocity, and it is being widely used in the industry.

### 3.3. Volume of green water on FPSO deck

Fig. 11 tracks the time history of volume of green water over the deck with and without the wall respectively. The figure shows that there are two peaks (or two green water events) for both two cases, where the first peak is significantly smaller than the second one. If the wall is mounted, the green water is accumulated around the corner between the deck edge and the wall, whereas the water volume in the case without the wall is more uniformly distributed along the deck. It means, if the FPSO is free to move, the stability of the FPSO with the wall is influenced by the green water more than that without the wall.

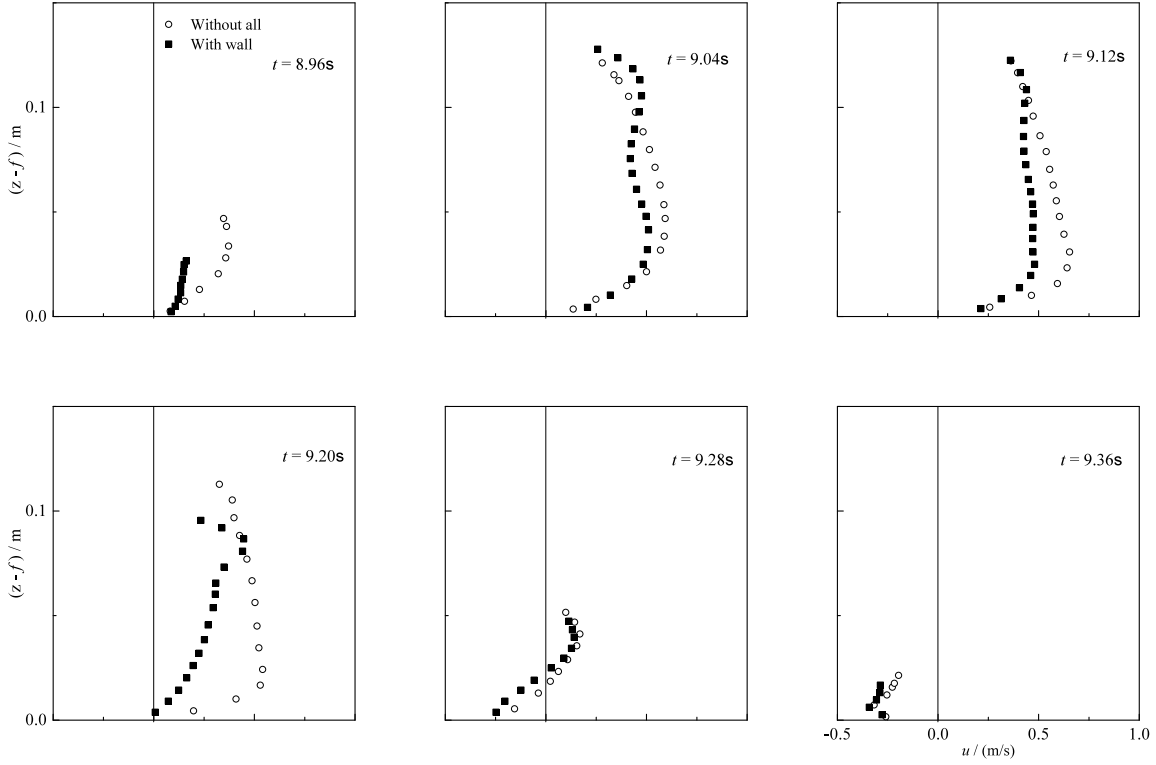


Figure 9: Comparison of  $u$  velocity distribution at the edge of deck for the cases with and without the wall in the second impact event

Based on the signals for wave maker motions provided in Greco (2001), the effect of wave height on the volume of water inundation over the deck without and with the wall is investigated, as shown in Fig. 12. From the figure, it is observed that with the larger wave height, the amount of green water certainly becomes larger. In addition, the maximum  $V_w/V_b$  in different wave heights for these two cases is almost the same.

Deck elevation is another key parameter for the volume of water inundation, and its effect is shown in Fig. 13. Compared to Fig. 12, it appears that the volume of green water on the deck seems to follow a similar trend by varying the deck elevation or the wave height. To confirm this, the relationship between  $(H - f)$  and the maximum  $V_w/V_b$  is shown in Fig. 14, which includes the results for both different wave heights and deck elevations. From the figure, it can be seen that a linear relationship nicely exists between  $(H - f)$  and the maximum  $V_w/V_b$  for both the cases with and without the wall. With this linear relationship, the occurrence of green water on the FPSO deck can be easily predicted for a selected group of wave height  $H$  and deck elevation  $f$ , which may be of great significance in the determination of wave height  $H$  and deck elevation  $f$  in industrial designs.

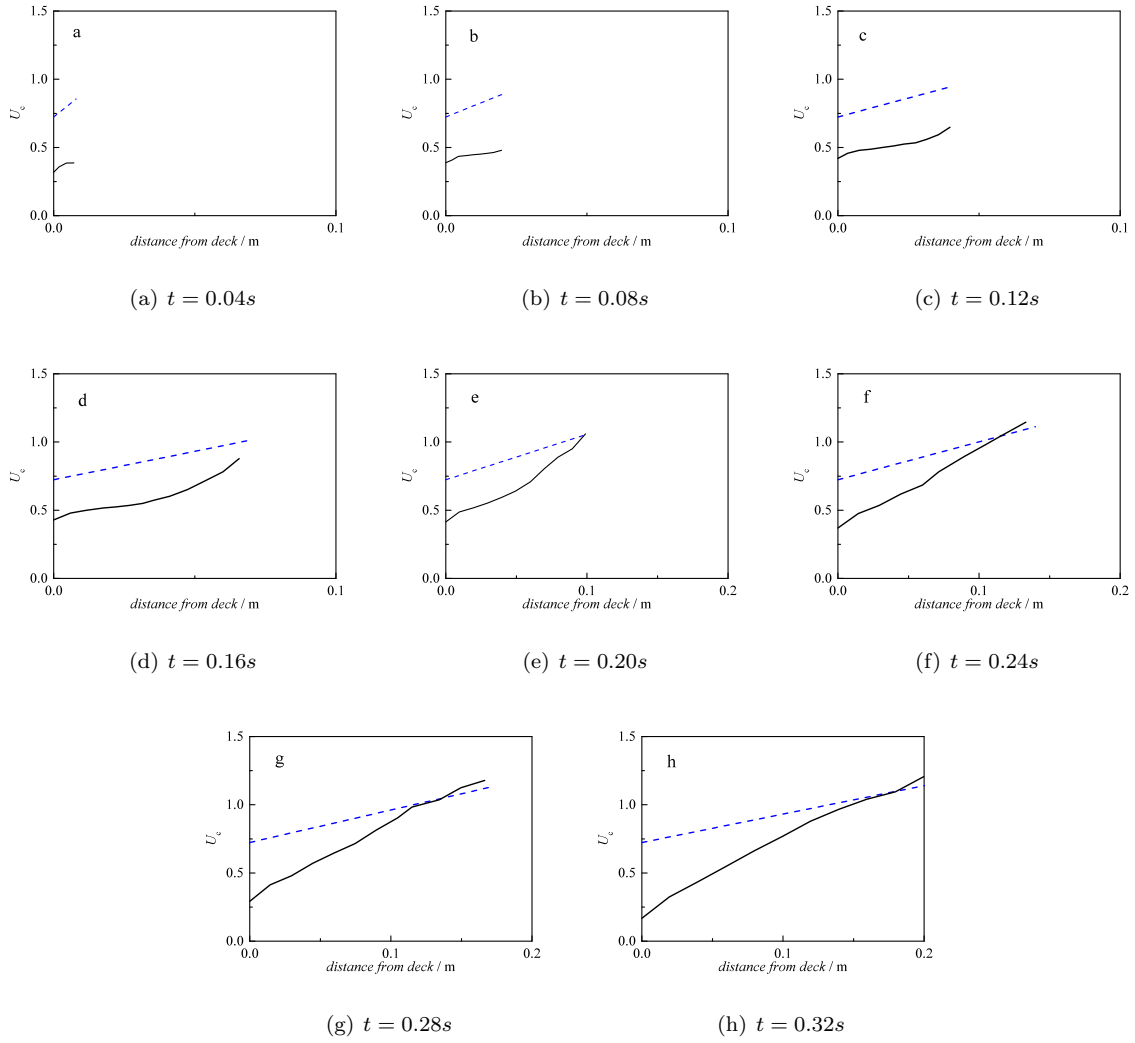


Figure 10: Comparison of velocity distribution along the fixed FPSO deck between the Ritter's solution (dash line) and numerical simulation (solid line) at various time instants

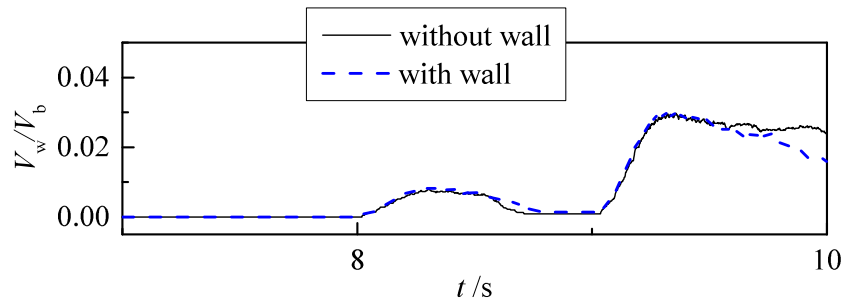
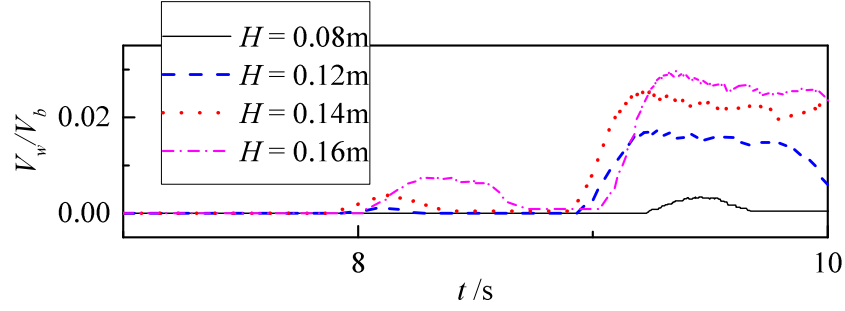
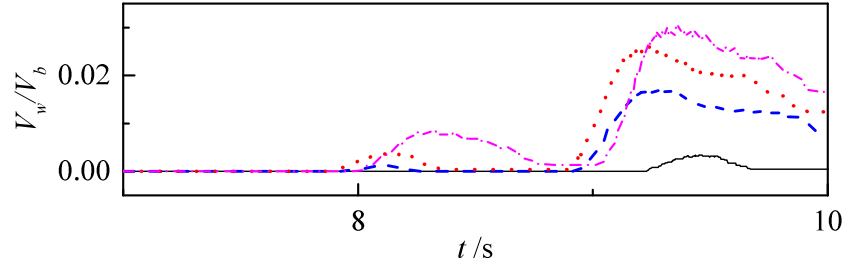


Figure 11: Time history of volume of water inundation over the deck with and without the wall.  $V_w$  and  $V_b$  are the volumes of green water and deck, respectively.



(a) without wall



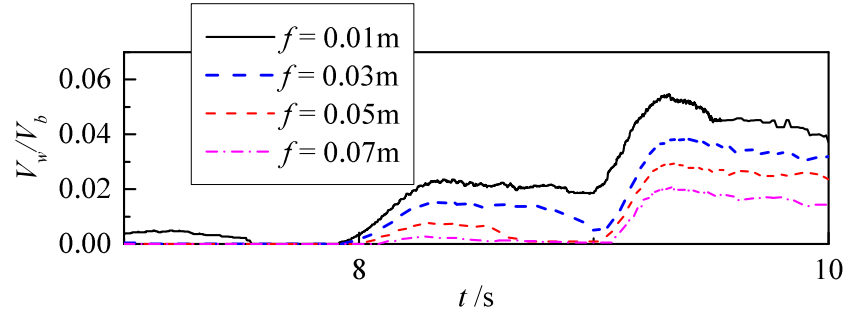
(b) with wall

Figure 12: Wave height effect on the volume of water inundation over the deck (a) without and (b) with the wall

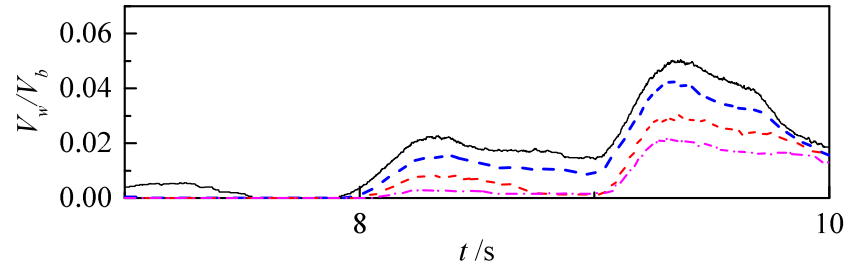
## 4. Green water on a fixed platform deck

### 4.1. Comparisons with experiment

As discussed above, offshore platform can be simplified to a thin plate, and the truss section supporting the platform can be ignored because it throws little hydrodynamic effect on the platform. In this section, the present numerical simulations will adopt the setup in the experiment of Cox and Ortega (2002) to carry out the study on this problem. Fig. 15 gives the sketch for the problem of green water over a fixed deck. As only the signal of voltage for the motion of wave paddle was given in Cox and Ortega (2002), different amplitudes of wave paddle motions have to be tried out in order to generate the same wave profile as in the experiment. Since it was to study the kinematics of one overtopping event, a short transient wave was chosen in the experiment that produced one large wave crest at the leading edge of the deck. In order to test the accuracy of the wave generation, wave elevations at two positions ( $x = 4.5m$  and  $x = 8.0m$ ) are tracked and compared with the experimental data in Cox and Ortega (2002), as shown in Fig. 16 for the case of pure wave propagation in the tank. It can be observed that the wave generated in the numerical simulation agrees considerably well with the experimental measurement, and the difference in maximum wave height between the present results and experimental data at both two locations is about 4%. In addition, when the transient wave propagates to the position at  $x = 8.0m$  where the leading edge of the fixed deck is located,

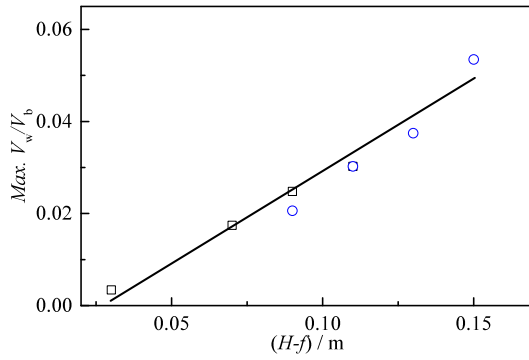


(a) without wall

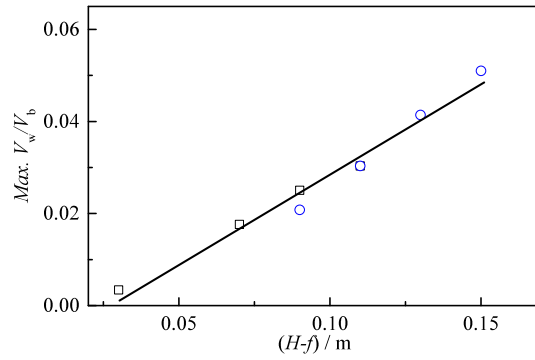


(b) with wall

Figure 13: Deck elevation effect on the volume of water inundation over the deck (a) without and (b) with the wall



(a) without wall



(b) with wall

Figure 14: Relationship between the maximum  $V_w/V_b$  and relative wave height  $(H - f)$  for the cases (a) without and (b) with the wall. The square symbol represents the data for various wave heights with  $f = 0.05m$ ; the circle symbol represents the data for various deck elevations with  $H = 0.16m$ . The solid line is the fitting curve for these scattered points.



the wave is focused to a maximum with about 20cm height, followed by a much smaller wave crest at around the time instant  $t = 10s$ .

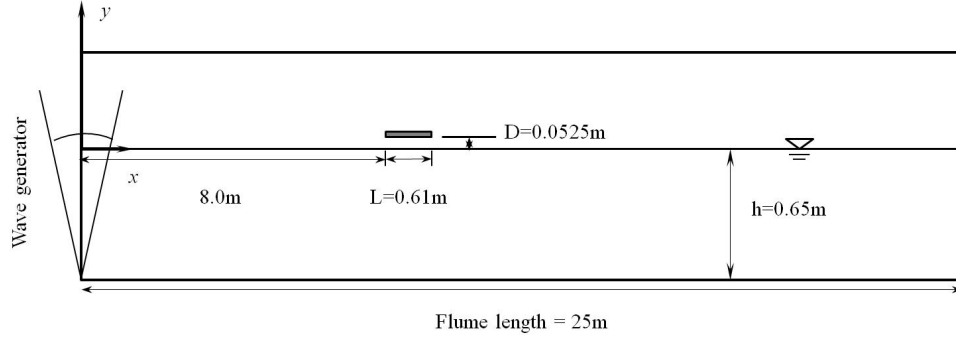
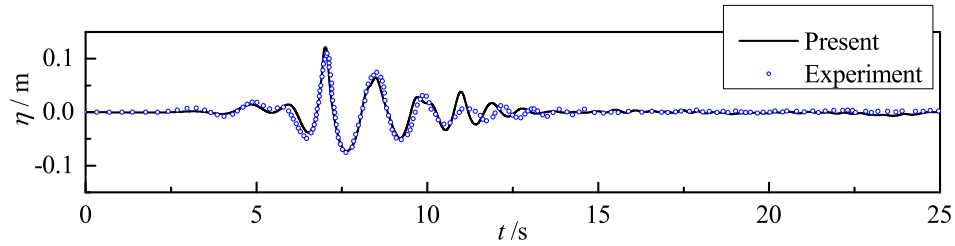
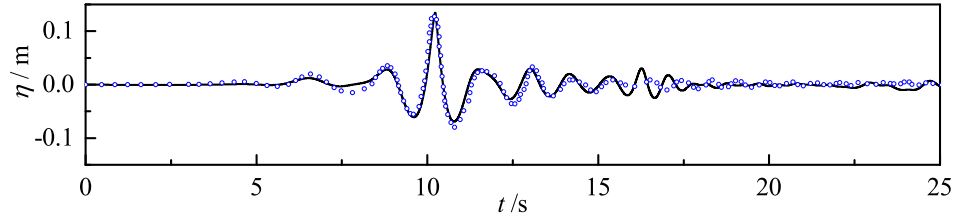


Figure 15: Sketch for the problem of green water over a fixed platform deck



(a)  $x = 4.5m$



(b)  $x = 8.0m$

Figure 16: Time history of wave elevations at two probes for the case of pure wave propagation

Next, the green water over the fixed platform deck is examined. As the convergence test has been conducted in the previous case of green water over a fixed FPSO deck, the present section only shows the convergent result directly, with the grid of  $0.02m \times 0.0025m$  around the deck. Near the free surface, adequate grids in the vertical direction (80 cells in one wave height) are generated as well to ensure the resolution in capturing the free surface. Fig. 17 shows the time history of wave elevations at three locations for the cases with the fixed platform deck. Compared to the wave elevation in the case without the fixed platform deck in Fig. 16(b), there is little difference in the wave crests and troughs when the deck is presented. It means that the deck exhibits little effect on the wave propagation. In addition, the numerical results present a good

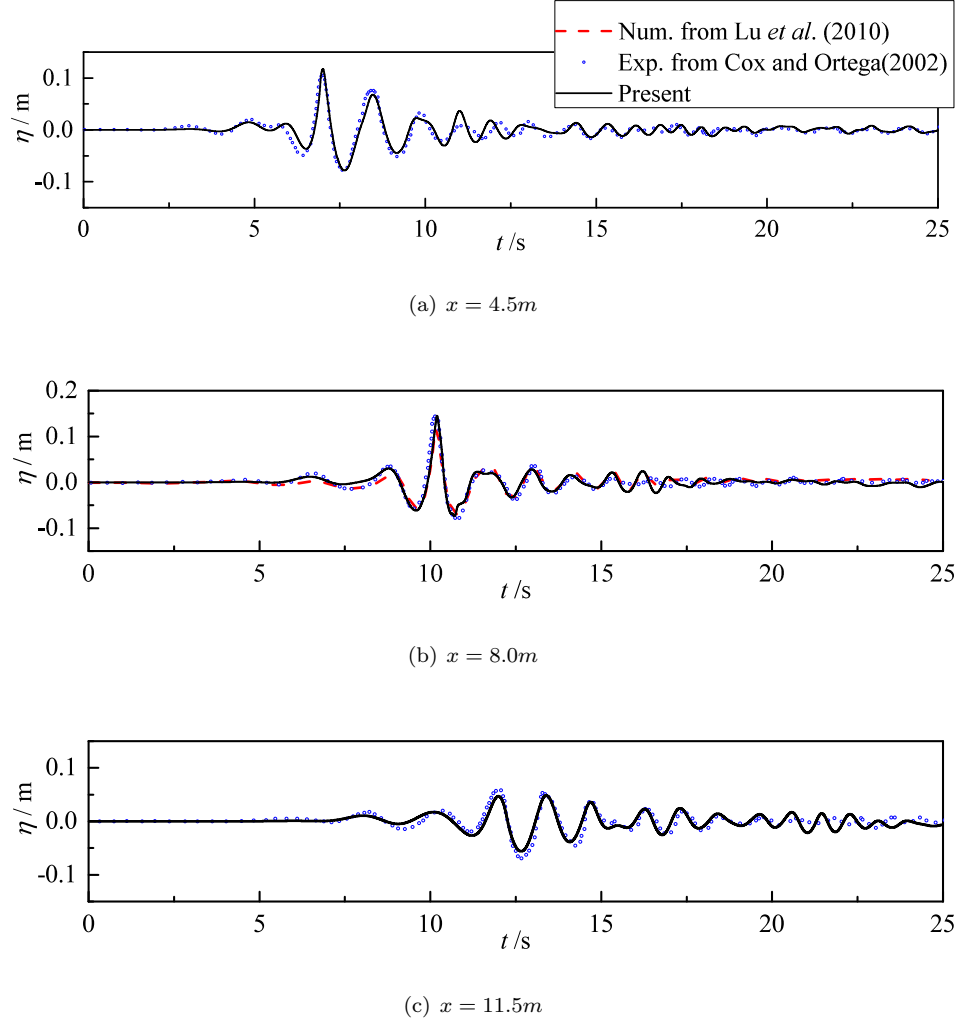


Figure 17: Time history of wave elevations at three probes for the case with the fixed deck

271 agreement with the experimental data, especially in the crests and troughs at all the three positions, which  
 272 is better than the comparison presented in Lu et al. (2010) where the generated wave was underestimated  
 273 due to the possible large numerical diffusion.

274 Fig. 18 presents the variation of horizontal velocity along the vertical direction at 12 different phases for  
 275 the case with the fixed deck at  $x = 8.0m$ . The effect of the structure on the velocity variation is obvious.  
 276 The fixed deck prevents the smooth distribution of the horizontal velocity. Individually, velocity distribution  
 277 on the deck still follows the exponential function approximately, while it almost remains the same below the  
 278 deck compared to the pure wave propagation. In general, the present numerical results obtain a considerably  
 279 good agreement with the experimental data. Again, comparison of the cross-sectional velocity ( $U_c$ ) between  
 280 the Ritter's solution and the present numerical result is shown in Fig. 19. Far away from the water front,  
 281 the Ritter's solution is obviously overestimated. However, closer to the water front, the Ritter's solution can

provide better results.

#### 4.2. Volume of green water on a platform deck

Similar to the case of green water on a FPSO deck, the volume of water inundation on the fixed platform deck is also examined in this section. Fig. 20 shows the effect of wave height and deck elevation on the volume of water inundation over the deck. In Fig. 20(a), the deck elevation is fixed at  $f = 0.0525m$ , while different deck elevations are investigated in Fig. 20(b) with the same wave height  $H = 0.222m$ . Here, due to the transient wave generation, the wave height  $H$  denotes the maximum wave height at  $x = 8.0m$ . For the case of  $f = 0.0525m$  in Fig. 20(a), the maximum volume ratio  $V_w/V_b$  can reach the value of 1.0 at larger wave height. In other word, the deck has to bear a large amount of water loads, which challenge the supporting structure, possibly leading to the destruction of the entire system. When the deck elevation  $f$  drops to  $0.0125m$  in Fig. 20(b), the deck can experience almost twice the water loads compared to that for  $f = 0.0525m$ . This figure also shows that the deck experiences a larger amount of green water loads in a longer time duration for the lower deck.

Furthermore, relationship between the relative wave height ( $H - f$ ) and the maximum volume ratio  $V_w/V_b$  is shown in Fig. 21. It is observed that a linear relationship exists in the considered range, which is consistent with the conclusion for the green water over a FPSO deck, by which the deck elevation can be predicted to avoid much water inundation when the extreme wave approaches to the deck.

## 5. Conclusions

In this paper, an improved immersed boundary method is applied to investigate the green water on a fixed deck. The complicated free surface is captured by the level set method in this numerical model, and a finite difference method of second-order accuracy is adopted to solve the flow field. Two different types of decks, a FPSO deck and a platform deck, are considered in this study. Extensive comparisons of the water surface elevation and pressure are conducted for the green water over both these two types of fixed decks with the physical experiments. Considerably good agreement can be achieved in all the comparisons between the experimental data and numerical results. More importantly, the present study also compares the velocity distribution along the deck with the Ritter's solution, which indicates that the Ritter's solution that is being widely used in the industry is more conservative than the numerical results, and is safer in the engineering design for both types of structures. In addition, another emphasis of the present study lies in the investigation of green water volume over the deck. It is revealed that for both the FPSO and platform decks, the amount of green water changes linearly with the relative wave height  $H - f$ , which is an important finding for the determination of deck elevation under a selected wave condition to avoid excessive volume of green water overtopping on structures.

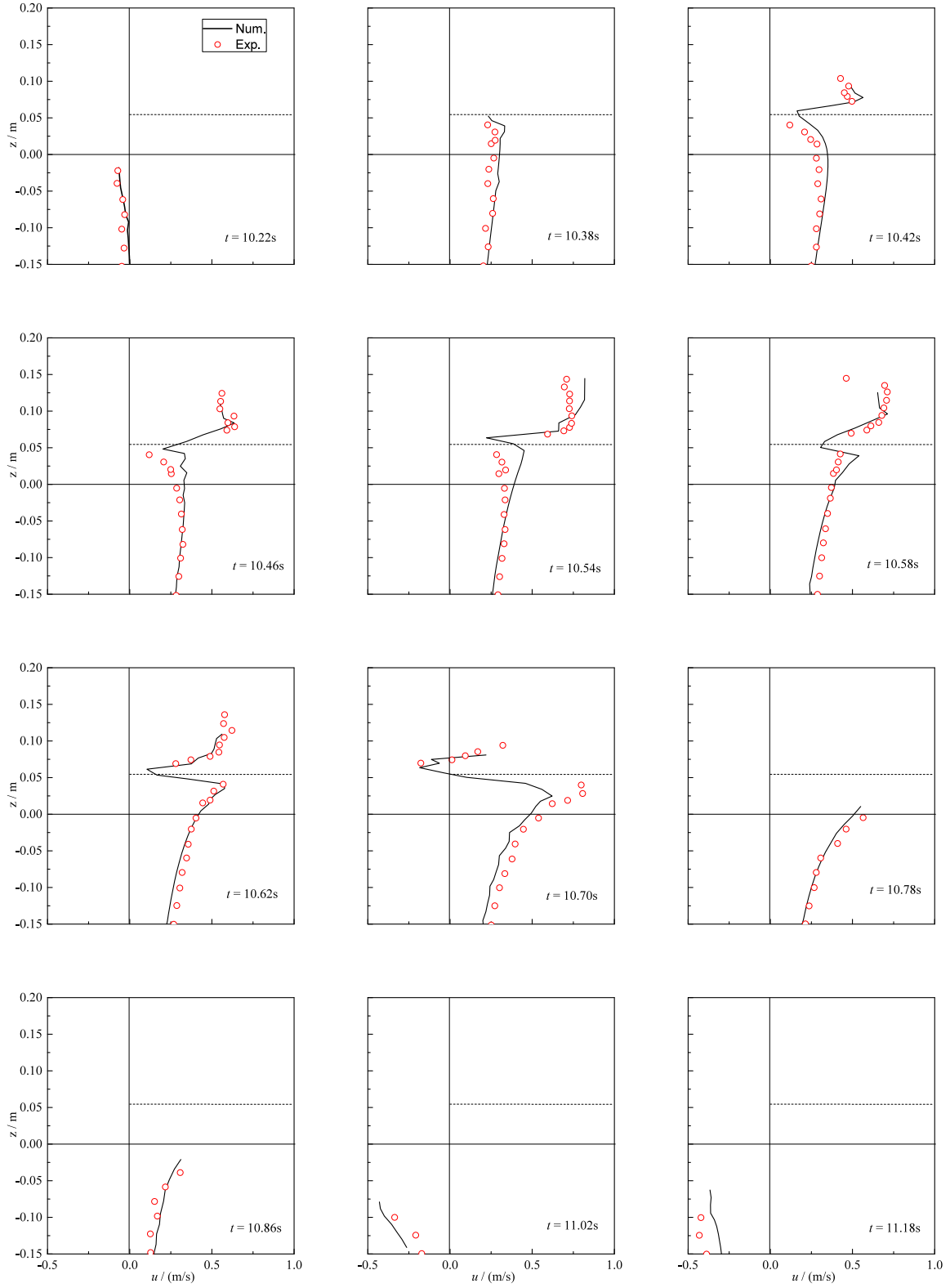


Figure 18: Comparison of the horizontal velocity for the cases with the fixed deck at various time instants. The dashed line shows the position of the fixed deck.

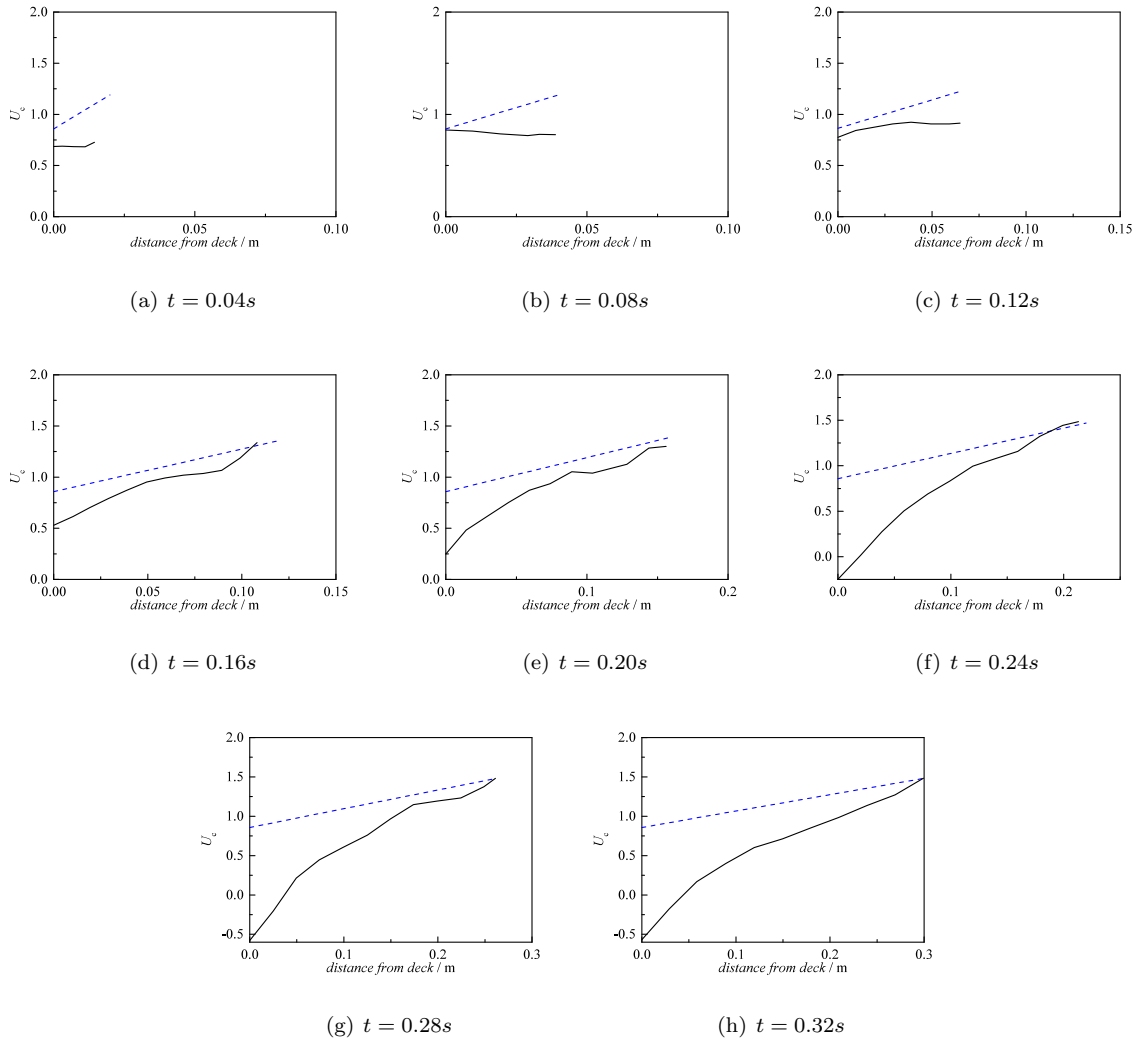
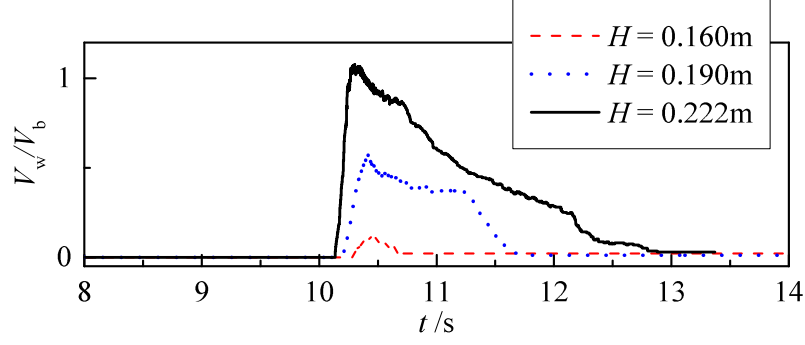


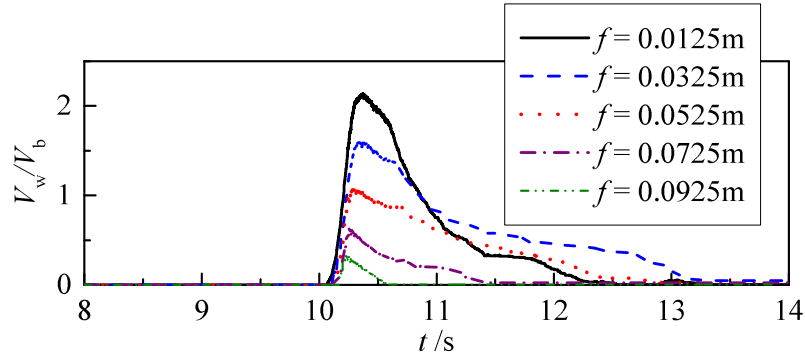
Figure 19: Comparison of velocity distribution along the fixed platform deck between the Ritter's solution (dash line) and numerical simulation (solid line) at various time instants

## References

- Archer, P. and Bai, W. (2015). A new non-overlapping concept to improve the hybrid particle level set method in multi-phase fluid flows, *Journal of Computational Physics* **282**: 317–333.
- Ariyaratne, K., Chang, K. A. and Mercier, R. (2012). Green water impact pressure on a three-dimensional model structure, *Experiments in Fluids* **53**(6): 1879–1894.
- Barcellona, M., Landrini, M., Greco, M. and Faltinsen, O. (2003). An experimental investigation on bow water shipping, *Journal of Ship Research* **47**(4): 327–346.
- Bea, R., Xu, T., Stear, J. and Ramos, R. (1999). Wave forces on decks of offshore platforms, *Journal of Waterway, Port, Coastal, and Ocean Engineering* **125**(3): 136–144.



(a)



(b)

Figure 20: Time history of volume of water inundation at (a) various wave heights and (b) different deck elevations

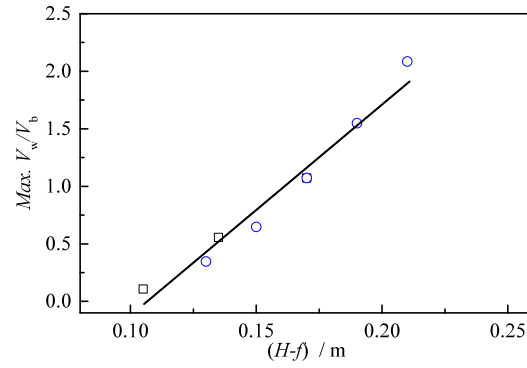


Figure 21: Relationship between the maximum  $V_w/V_b$  and relative wave height  $(H - f)$  for green water on a fixed platform deck. The square symbol represents the data for various wave heights with  $f = 0.0525m$ ; the circle symbol represents the data for various deck elevations with  $H = 0.222m$ . The solid line is the fitting curve for these scattered points.

- Buchner, B. (1995). The impact of green water on FPSO design, *The 27th Offshore Technology Conference*, Houston, Texas, USA, pp. 45–57.
- Cox, D. T. and Ortega, J. A. (2002). Laboratory observations of green water overtopping a fixed deck, *Ocean Engineering* **29**(14): 1827–1840.
- Cox, D. T. and Scott, C. P. (2001). Exceedance probability for wave overtopping on a fixed deck, *Ocean Engineering* **28**(6): 707–721.
- Denson, K. H. and Priest, M. S. (1971). Wave pressures on the underside of a horizontal platform, *Proc. Offshore Technology Conference*, Vol. 1, Offshore Technology Conference, Houston, Texas, pp. 555–570.
- French, J. (1969). Wave uplift pressures on horizontal platforms, *Report KH-R-19*, Division of Engineering and Applied Science, California Institute of Technology, Pasadena, California.
- Gómez-Gesteira, M., Cerqueiro, D., Crespo, C. and Dalrymple, R. A. (2005). Green water overtopping analyzed with a SPH model, *Ocean Engineering* **32**(2): 223–238.
- Greco, M. (2001). *A two-dimensional study of green-water loading*, PhD thesis, Norwegian University of Science and Technology, Trondheim, Norway.
- Jiang, G. and Peng, D. (2000). Weighted ENO schemes for Hamilton-Jacobi equations, *SIAM Journal on Scientific Computing* **21**(6): 2126–2143.
- Kaplan, P. (1992). Wave impact forces on offshore structures: re-examination and new interpretations, *Proc. Offshore Technology Conference*, Vol. 1, Houston, Texas, pp. 79–88.
- Lai, C. and Lee, J. (1989). Interaction of finite amplitude waves with platforms or docks, *Journal of Waterway, Port, Coastal and Ocean Engineering*, ASME **115**(1): 19–39.
- Lauber, G. and Hager, W. H. (1998). Experiments to dambreak wave: Horizontal channel, *Journal of Hydraulic Research* **36**(3): 291–307.
- Lee, H. H., Lim, H. J. and Rhee, S. H. (2012). Experimental investigation of green water on deck for a CFD validation database, *Ocean Engineering* **42**(Supplement C): 47–60.
- Lu, H., Yang, C. and Lohner, R. (2010). Numerical studies of green water impact on fixed and moving bodies, *Proceedings of the Twentieth International Offshore and Polar Engineering Conference*, Beijing, China, pp. 393–400.
- Mohd-Yusof, J. (1997). Combined immersed boundary/B-spline method for simulations of flows in complex geometries, *Technical report*, Center Annual Research Briefs, NASA Ames/Stanford University.
- Nielsen, K. B. and Mayer, S. (2004). Numerical prediction of green water incidents, *Ocean Engineering* **31**(3): 363–399.

- 354 Qin, H., Tang, W., Hu, Z. and Guo, J. (2017). Structural response of deck structures on the green water  
355 event caused by freak waves, *Journal of Fluids and Structures* **68**: 322–338.
- 356 Ritter, A. (1892). Die fortpflanzung de wasserwellen, *Zeitschrift Verein Deutscher Ingenieure* **36**(33): 947–  
357 954.
- 358 Ryu, Y., Chang, K. A. and Mercier, R. (2007a). Application of dam-break flow to green water prediction,  
359 *Applied Ocean Research* **29**(3): 128–136.
- 360 Ryu, Y., Chang, K. A. and Mercier, R. (2007b). Runup and green water velocities due to breaking wave  
361 impinging and overtopping, *Experiments in Fluids* **43**(4): 555–567.
- 362 Shao, S., Ji, C., Graham, D. I., Reeve, D. E., James, P. W. and Chadwick, A. J. (2006). Simulation of wave  
363 overtopping by an incompressible SPH model, *Coastal Engineering* **53**(9): 723–735.
- 364 Silva, D. F. C., Esperana, P. T. T. and Coutinho, A. L. G. A. (2017). Green water loads on FPSOs exposed  
365 to beam and quartering seas, Part II: CFD simulations, *Ocean Engineering* **140**: 434–452.
- 366 Stansby, P. K., Chegini, A. and Barnes, T. C. D. (1998). The initial stages of dam-break flow, *Journal of*  
367 *Fluid Mechanics* **374**: 407–424.
- 368 Xiao, L., Tao, L., Yang, J. and Li, X. (2014). An experimental investigation on wave runup along the  
369 broadside of a single point moored FPSO exposed to oblique waves, *Ocean Engineering* **88**(0): 81–90.
- 370 Xiao, L., Yang, J., Tao, L. and Li, X. (2015). Shallow water effects on high order statistics and probability  
371 distributions of wave run-ups along FPSO broadside, *Marine Structures* **41**: 1–19.
- 372 Yan, B., Bai, W. and Quek, S. T. (2018). An improved immersed boundary method with new forcing point  
373 searching scheme for simulation of bodies in free surface flows, *Communications in Computational Physics*  
374 **24**(3): 830–859.
- 375 Yilmaz, O., Incecik, A. and Han, J. C. (2003). Simulation of green water flow on deck using non-linear dam  
376 breaking theory, *Ocean Engineering* **30**(5): 601–610.